

Recent advances in remote sensing of extra-tropical Rossby waves

P. Cipollini, P.G. Challenor, D. Cromwell, K.L. Hill[†], G.D. Quartly, and I.S. Robinson
Southampton Oceanography Centre, Empress Dock,
Southampton, Hants, SO14 3ZH, UK
email: *cipo@soc.soton.ac.uk*

[†]Now at University of Victoria, Canada

Abstract

Rossby waves are important physical processes transmitting information across ocean basins and affecting western boundary currents. In recent years there have been a wide number of papers covering altimetric observations of Rossby waves in many basins. We briefly review some of these findings, and then describe the various signal processing techniques that may be used to extract information on the characteristics of Rossby waves. We illustrate with both height and temperature data from the South Indian Ocean and show how such results can lead to both better theoretical and numerical models.

1. Introduction

Oceanic Rossby waves (otherwise called 'planetary waves') are large-scale propagating features that owe their nature to being in a fluid co-rotating with the solid earth. Although their surface manifestation might appear slight — a raising of the mean sea surface height (SSH) by a few centimetres and an increase in sea surface temperature (SST) by a fraction of a degree — they are important for the effects they have on other oceanic processes. Rossby waves travel westward at speeds of the order of 1 to 10 km day⁻¹ (the speed increases equatorward) carrying information from their source region, and they set the response time of processes in the west of basins to changes occurring in the east.

Possible stimuli include strong changes in wind forcing, variations in currents and the passage of poleward-propagating Kelvin waves. The resultant baroclinic Rossby waves have a velocity structure in the meridional direction, and change the height of the thermocline by tens of metres. Their effect on reaching the west is to intensify the Western Boundary Current, and possibly to alter its position and thus change the ocean's modification of the atmosphere (*Jacobs et al.*, 1994).

To understand better the complex ocean-atmosphere system, and especially the likelihood of significant climate change, one needs a good understanding of Rossby waves — where they occur, their amplitude, and particularly their speed of propagation, which determines the timescale for ocean-atmosphere feedback. First, in section 2 we review previous results. Section 3 then describes the preliminary processing of SSH data, with section 4 discussing various signal processing techniques. A corresponding analysis for SST is given in section 5. Section 6 relates the revisions to Rossby wave theory in response to such observations and contrasts the results with output from a numerical model. The final section summarises the observations and provides hints as to future research.

2. Previous observations

Despite the theoretical formulation of Rossby waves being proposed by Carl Gustav Rossby in the 1930s, observations of oceanic Rossby waves are confined to the last 30 years. This is due to their small surface signal and large wavelength (hundreds to thousands of kilometres), which, until the advent of accurate global observations from space, precluded their detection in all but a few regions of strong signals and intensive sampling. The advent of altimeters able to measure SSH to a precision of a few centimetres enabled a number of authors to determine Rossby waves in specific locations (e.g. *Tokmakian and Challenor (1993)* using Geosat data). As the accuracy of altimeters improved, Rossby waves were found to be a global phenomenon and *Chelton and Schlax (1996)* using TOPEX/Poseidon altimeter data, noted that at mid-latitudes the propagation speeds were much faster than expected from the simple linear theory.

Rossby waves have been hard to observe in SST, on account of the need for datasets large in both spatial and temporal extent, and with little remnant contamination by clouds. *Van Woert and Price (1993)* observed Rossby waves in AVHRR data near the Hawaiian archipelago, and *Cipollini et al. (1997)*, using ATSR data, found a strong signal near the region of the Azores Current in the North Atlantic.

3. Rossby waves in SSH data

Sea surface height (SSH) data from TOPEX/Poseidon are provided every 5.8 km (1s along track); we apply the standard corrections for atmospheric delay, tides and sea state bias (see *Cipollini et al., 1997* for details) and calculate SSH residuals with respect to the mean for 1993-95. The data are then interpolated onto a $1^\circ \times 1^\circ$ grid using Gaussian weighting, with a full width half maximum of 150 km and a search radius of 200 km. Given that the accuracy of the original altimeter data is of the order of a few centimetres, the error of the gridded average will be close to 1 cm. For a particular case study, we consider the South Indian Ocean at 25°S ; this corresponds to a region within the southern subtropical gyre, with no strong currents. The strongest cause of SSH variability is the basin-wide changes caused by the annual cycle of thermal expansion and cooling of the surface waters. To remove this signal we apply a high-pass filter to leave anomalies relative to the local mean. The results are displayed in Figure 1.

Diagonal alignment of crests and troughs (positive and negative anomalies respectively) run from west to east, taking about 30 months to travel 50° of longitude; this corresponds to a mean velocity of 5.5 km day^{-1} . Quantitative estimates of speed using advanced signal processing techniques are discussed in the succeeding

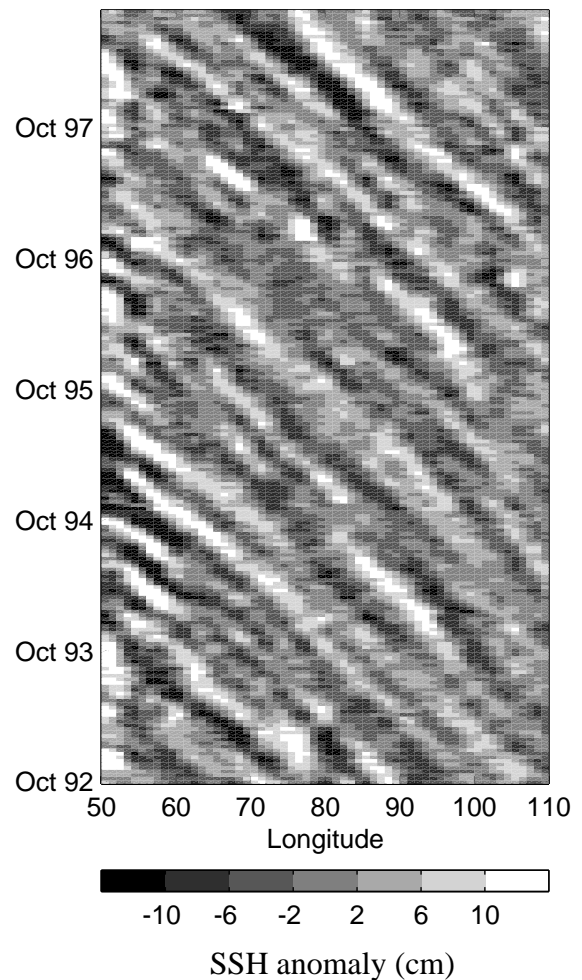


Fig. 1: Hovmöller diagram of SSH anomalies at 25°S in the Indian Ocean after high-pass zonal filtering.

section; however it can be seen from Fig. 1 that the velocities are slightly greater in the western half of the basin.

4. Analysis techniques

Figure 2a shows a Fourier transform of the data, showing that the dominant wavelength and period are 1600 km and 350 days, but with significant power at its second harmonic (800km and 175 days). Both peaks correspond closely to a propagation speed of 6 km day^{-1} (shown by the dotted line). However the original data do not reveal a *regular* pattern of evenly-spaced constant-speed features of equal amplitude. There are changes in speed both with location and time, probably in response to varying stratification of the water column (which affects the vertical structure and thus the restoring force of the Rossby waves). Also individual Rossby waves ('solitons') show a wide range of amplitudes, according to the forcing that had instigated them.

An alternative analysis technique is the Radon transform (Deans, 1983) that simply extracts information on alignments within the data, without assuming regularity. This technique yields an estimate of the 'power' associated with a given propagation speed (see Cipollini *et al.*, 1999), without separately determining wavelength or period. The resultant spectrum (Fig. 2b) also shows the dominant speed to be close to 6 km day^{-1} .

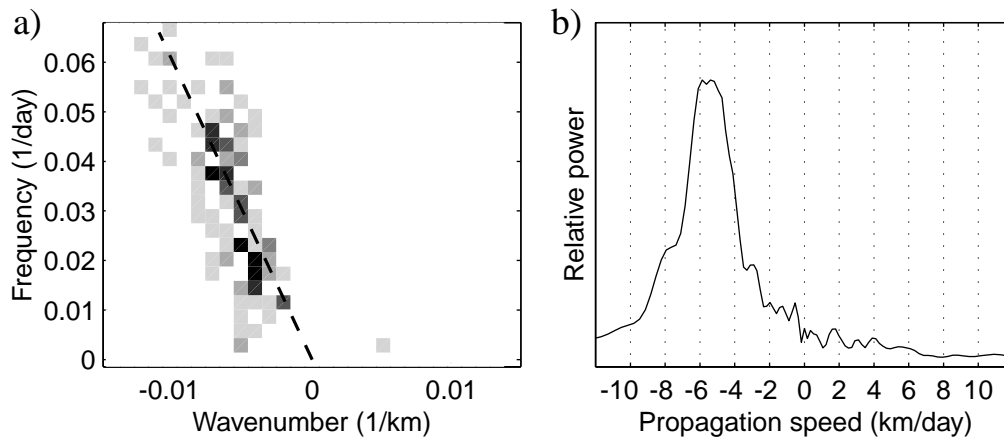


Fig. 2: Spectral analysis of data in Fig. 1. a) Fourier analysis, with darker colours representing more energy (added dashed line indicates all signals with a propagation speed of 6 km day^{-1}). b) Strength of signal for various speeds, determined from Radon transform.

However the spectral estimate appears smeared, with 2 closely spaced peaks at 5.8 and 5.3 km day^{-1} , due to the different dominant speeds in the western and eastern halves of Fig. 1. There is also a small local maximum at 2.9 km day^{-1} . To obtain a more 'uniform' dataset we may limit it in space and/or time and apply the processing to this subset. Clearly there is a compromise between uniformity (best for small datasets) and resolution (improved by larger series of data). In Fig. 3 we show specimen results for division of the original dataset into 15° by 12-month segments. The scaling is the same for each sub-plot, showing that the magnitude of Rossby waves at a given location may change by a factor of two between years. Several of the sub-plots also show a peak at 0 km day^{-1} corresponding to stationary features; there is no such signal in the analysis for the period as a whole (Fig. 2b) since the mean SSH anomaly at each location is close to zero. The series of Radon transform analyses does show the subtle change in propagation speed, with some of the peaks

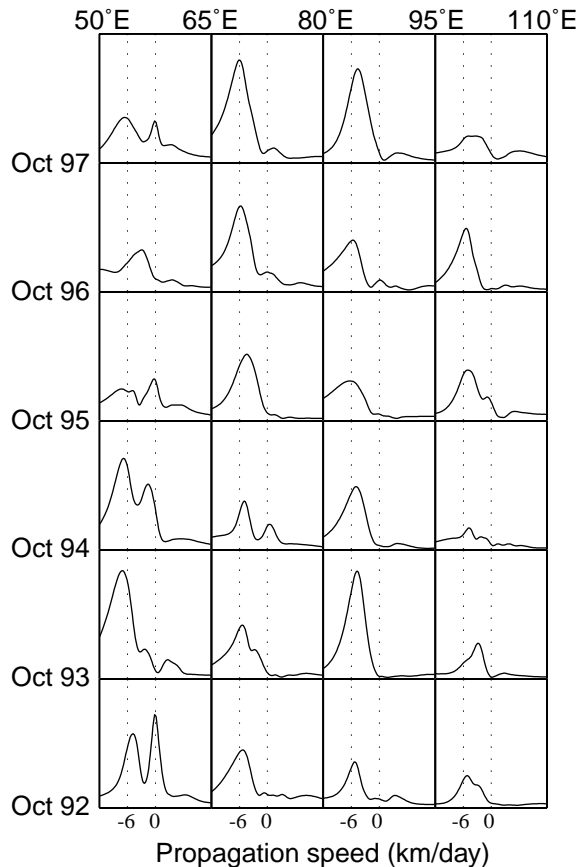


Fig. 3: Speed plots from Radon transform of individual 15° by 12-month segments of the data shown in Fig. 1. (All sub-plots have the same abscissa and ordinate range, with the dashed lines indicating speeds of -6 and 0 km day^{-1} .)

Van Woert and Price (1993) and Cipollini *et al.* (1997) had noted Rossby waves in SST at specific locations; however it is only more recently that Hill *et al.* (2000) have shown their ubiquity, taking advantage of the accurate calibration of the ATSR instrument. Its accuracy for instantaneous 1km^2 pixels is 0.3K (Mutlow *et al.*, 1994; Forrester and Challenor, 1995) but the errors are much less for the $0.5^\circ \times 0.5^\circ$ monthly averaged product that we use here.

Figure 4a shows a Hovmöller diagram for the SST values over the same section as Fig. 1. [Again a high-pass filter has been invoked to remove basin-scale seasonal variations.] Distinct diagonal alignments can be seen once more. The results of the Radon transform are shown in Fig. 4b. Most (9 out of 12) of the segments show a dominant speed of around 4 km day^{-1} ; combining these together gives a mean speed of 4.0 km day^{-1} (s.d.= 0.65 km day^{-1} , and the standard error of the mean is thus 0.22 km day^{-1}); the other three have a mean of 5.8 km day^{-1} (s.d. = 0.38 km day^{-1}). The results of the SSH analysis are that 19 of the 24 subsets had a peak between 5 and 6 km day^{-1} , with a mean of 5.5 km day^{-1} (s.d. = 0.79 km day^{-1} , and thus standard error is 0.18 km day^{-1}).

in the 1st (left-hand) column being to the left of the dotted line (i.e. greater than 6 km day^{-1}) and those in the other columns being to the right.

Another technique for dealing with spatial and temporal modulation of Rossby waves in a 2-D Hovmöller plot is to use the wavelet transform (e.g. Wang *et al.*, 1998), or alternatively one may fit individual features with a translating Gaussian profile that evolves slowly in time. However we do not have space to illustrate either of these techniques here. If there are strong meridional density gradients or bathymetric slopes, the Rossby waves will have a non-zonal component to their propagation. In such a case individual Rossby waves will not lie in a single latitudinal section, but follow a slant path through a cuboid of data (lat \times lon \times time). To extract such a feature we need a 3-D Radon transform (Cipollini *et al.*, 2000; Challenor *et al.*, 2000).

5. Rossby waves in SST data

Given that Rossby waves involve a perturbation to the density profile of the water column, and that temperature is an important parameter affecting density, it seems plausible that Rossby waves should have a thermal signature. For such to be discerned from satellites it is necessary that the skin layer is not isolated from the bulk variation and that the signal is greater than the precision of the satellite measurement.

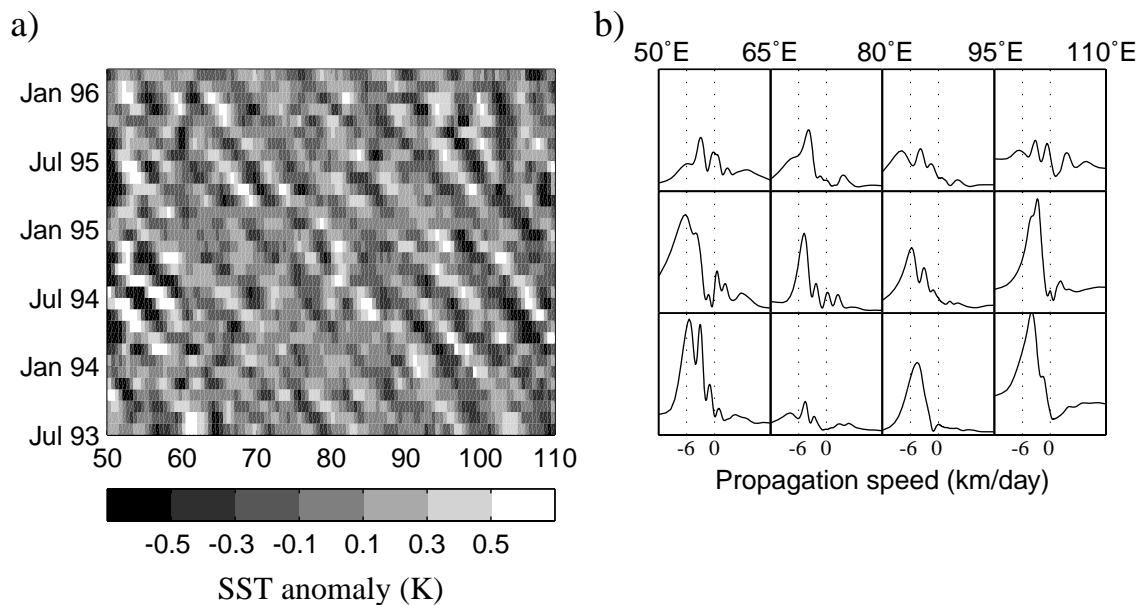


Fig. 4: Analysis of SST data. a) Hovmöller diagram for same longitudinal range as in Fig. 1. b) Speed plots for individual 15° by 12-month segments of the data (with dashed lines again indicating -6 and 0 km day^{-1}).

6. Rossby waves in theory and models

With the multitude of SSH analyses in recent years it became clear that the measured speeds were significantly greater than that expected from the standard linear theory. This led to revisions of Rossby wave theory to include the effects of varying current profile (Killworth *et al.*, 1997) and bathymetry (Killworth and Blundell, 1999). These improvements changed the predicted Rossby wave speed at 25°S in the Indian Ocean from 4.0 km day^{-1} to 5.1 km day^{-1} , providing good agreement with our SSH results, but not the SST ones. It is conjectured that the temperature signal is responding primarily to the second baroclinic mode rather than the first. It has also been suggested that complex atmospheric feedback means that the observed SSH signal may be the result of a coupled ocean-atmosphere Rossby wave (White *et al.*, 1998).

It is also instructive to examine model output for Rossby waves, not so as to come up with another theoretical 'prediction', but to test how well they reproduce reality. Today numerical models are able to reproduce well the mean ocean circulation and mesoscale variability. Rossby waves should be present too, without the need to be explicitly written in — if the standard physical processes are coded well in a high-resolution model, then Rossby waves will be one of the results. Rossby waves are indeed found in output from many models, but Cipollini *et al.* (2000), in a study of isopycnic models of the N. Atlantic, found the Rossby waves to be slow and weak in amplitude. The slow speed is indicative that the density or velocity profile in the model is not close enough to that of the real world; whilst the small amplitude indicates that the monthly mean climatological forcing used is not able to excite strong Rossby waves. We have yet to test whether changing to real 6-hourly forcing will remove this discrepancy. Cipollini *et al.* (2000) also noted that the Rossby wave propagation in a coarse model was very different to its fine-scale counterpart.

7. Conclusions and further work

Rossby waves are important physical mechanisms linking actions between the east and west of ocean basins and thus setting a response time for the oceans. Their surface signature is small, but the great improvements in satellite altimetry and radiometry during the past decade have enabled Rossby waves to be detected in most locations. Using a section at 25°S we have demonstrated the use of Fourier and Radon transforms

for the recovery of wave information. Such observations have prompted amendments to Rossby wave theory to account for the greater speeds than originally expected, and at the same time are also providing a severe test of numerical models' ability to respond correctly to interannual changes in the forcing at the east of a basin.

In some locations Rossby waves can be seen in SSH, SST and ocean colour (see *Cipollini et al.*, this volume), with different speeds according to their different baroclinic modes. Because of the different density profiles associated with each, together they offer the intriguing possibility of inferring the deep density structure from satellite observations of the surface.

Acknowledgements

We thank Helen Snaith for the provision of the altimeter processing software.

References

- Challenor, P.G., P. Cipollini and D. Cromwell, 2000, Use of the 3-D Radon transform to examine the properties of oceanic Rossby, *submitted to J. Atmos. Oceanic. Tech.*
- Chelton, D.B. and M.G. Schlax, 1996, Global observations of oceanic Rossby waves, *Science*, **272**, 234-238.
- Cipollini, P., D. Cromwell, M.S. Jones, G.D. Quartly and P.G. Challenor, 1997, Concurrent altimeter and infrared observations of Rossby wave propagation near 34°N in the northeast Atlantic, *Geophys. Res. Lett.*, **24**, 889-892.
- Cipollini, P., D. Cromwell and G.D. Quartly, 1999, Observations of Rossby wave propagation in the northeast Atlantic with TOPEX/POSEIDON altimetry, *Adv. in Space Res.*, **22**, 1553-1556.
- Cipollini, P., D. Cromwell, G.D. Quartly and P.G. Challenor, 2000, Remote sensing of oceanic extra-tropical Rossby waves, *Chap. 6 of "Satellites, Oceanography and Society" (edited by D. Halpern)* p. 99-123, [Elsevier].
- Deans, S.R., 1983, *The Radon transform and some of its applications*, [John Wiley, New York]
- Forrester, T.N. and P.G. Challenor, 1995, Validation of ATSR sea surface temperatures in the Faeroes region, *Int. J. Rem. Sensg.*, **16**, 2741-2753.
- Hill, K.L., I.S. Robinson and P. Cipollini, 2000, Propagation characteristics of extratropical planetary waves observed in the global ATSR sea surface temperature record, *J. Geophys. Res.* (in press).
- Jacobs, G.A., H.E. Hurlburt, J.C. Kindle, E.J. Metzger, J.L. Mitchell, W.J. Teague and A.J. Wallcraft, 1994, Decade-scale trans-Pacific propagation and warming effects of an El Niño anomaly, *Nature*, **370**, 360-363.
- Killworth, P.D., D.B. Chelton and R. de Szoeke, 1997, The speed of observed and theoretical long extra-tropical planetary waves, *J. Phys. Oceanogr.*, **27**, 1946-1966.
- Killworth, P.D. and J. R. Blundell, 1999, The effect of bottom topography on the speed of long extra-tropical planetary waves, *J. Phys. Oceanogr.*, **29**, 2689-2710.
- Mutlow, C.T., A.M. Závody, I.J. Barton and D.L.T. Llewellyn-Jones, 1994, Sea surface temperature measurements by the Along-Track Scanning Radiometer on the ERS-1 satellite: Early results, *J. Geophys. Res.*, **99**, 22575-22588.
- Tokmakian, R.T. and P.G. Challenor, 1993, Observations in the Canary Basin and the Azores Frontal region using Geosat data, *J. Geophys. Res.*, **98**, 4761-4773.
- van Woert, M.L. and J.M. Price, 1993, Geosat and Advanced Very High Resolution Radiometer observations of oceanic planetary waves adjacent to the Hawaiian islands, *J. Geophys. Res.*, **98**, 14619-14631.
- Wang, L., C. Koblinsky, S. Howden and B. Beckley, 1998, Large-scale Rossby wave in the mid-latitude South Pacific from altimetry data, *J. Geophys. Res.*, **25**, 179-182.
- White, W.B., Y. Chao and C.-K. Tai, 1998, Coupling of biennial oceanic Rossby waves with the overlying atmosphere in the Pacific basin, *J. Phys. Oceanogr.*, **28**, 1236-1251.